

Simultaneous Measurement of Viscoelasticity and Electrical Conductivity of an Electrorheological Fluid

Xiao-Dong Pan and Gareth H. McKinley*

*Division of Engineering and Applied Sciences, Harvard University,
Cambridge, Massachusetts 02138*

Received October 10, 1997. In Final Form: January 12, 1998

Simultaneous measurements of viscoelasticity and electrical conductivity are performed to study the dynamic characteristics of structures formed in a highly concentrated electrorheological suspension under a dc electric field of 1.8 kV/mm. Small amplitude oscillatory shear measurements reveal that there is no direct correlation between the elastic modulus and the electrical conductivity of the suspension. A significant increase in conductivity is observed following large amplitude oscillatory shear and, in this case, the linear elastic modulus is also substantially enhanced. These observations are interpreted according to the concept of *contact disorder* arising from the anisotropic shape of the particulate phase.

Electrorheological (ER) fluids^{1–3} are concentrated suspensions of fine polarizable particles in an insulating liquid. The stress transfer properties of ER fluids can be rapidly and reversibly changed with a strong external electric field ($E_0 \sim 1.0$ kV/mm). The potential use of ER materials in achieving real-time feedback control has been hindered largely by the insufficient material strength presently attainable. Although it is generally accepted that the observed dramatic change in rheological properties of ER materials originates from the formation of chainlike or columnar structures in the suspensions, which in turn is due to electric-field-induced polarization interactions among particles, the underlying mechanisms of the ER response are not yet fully understood. Assorted polarization models,^{4–6} a conduction model,^{7,8} and a water-bridge model⁹ have been proposed for understanding the ER response; however, we still lack definitive guidelines for improving the quality of ER materials.

In this Letter we present some unique results from simultaneous measurements of the dynamic modulus ($G^* = G' + iG''$) and electrical conductivity (σ) of an ER material under a strong dc electric field. As the oscillatory strain amplitude γ_a is gradually increased, the structures in the suspension are progressively disrupted and associated variations in both G^* and σ of the ER material should develop. This information can help us understand the nature of the interactions among particles forming the internal structures which is essential to optimizing ER materials.

Simultaneous measurements of G^* and σ under oscillatory shear strain have been made in the past on carbon-black-filled natural rubbers¹⁰ or carbon-black-reinforced vulcanizates (in weak dc electric fields 1–3 V/cm)¹¹ to study the effect of carbon black structures inside these

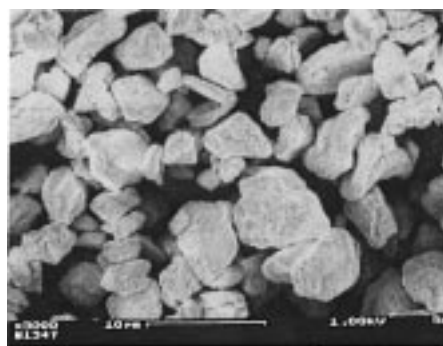


Figure 1. A SEM image of the carbonaceous particles. The scaling bar near the bottom denotes 10 μm .

materials. It was found that up to a strain amplitude $\gamma_a \sim 1.0$, the conductivity σ and the elastic modulus G' decreased with increasing γ_a in a roughly similar way, although the decline in G' started at a smaller γ_a than the decrease in σ .

The dynamic responses of the electric-field-induced structures in ER suspensions under imposed oscillatory shear have previously been probed either by employing a two-dimensional light scattering technique¹² or via measuring the dielectric constant of the suspension.¹³ However, simultaneous measurement of G^* and σ can definitely help in clarifying the role of electrical conduction in the ER response.

The specific ER fluid used in this study is a commercial ER fluid from Bridgestone (F569HT). It is claimed to be anhydrous and consists of carbonaceous particles dispersed in a silicone oil. This ER fluid exhibits a constant ER effect over a wide temperature range (tested from -40 to 120 °C), excellent durability at high temperature, similar activity under both dc and ac (~ 50 Hz) fields, and high ER effect at low current density.¹⁴

Examination of scanning electron microscopy (SEM) images of the carbonaceous particles shows that they have irregular angular shapes with sharp facets (Figure 1) and a size distribution mainly in the range of 1–10 μm . The

- (1) Block, H.; Kelly, J. P. *J. Phys. D: Appl. Phys.* **1988**, *21*, 1661.
- (2) Halsey, T. C. *Science* **1992**, *258*, 761.
- (3) Zukoski, C. F. *Annu. Rev. Mater. Sci.* **1993**, *23*, 45.
- (4) Anderson, R. A. In *Proceedings of the International Conference on Electrorheological Fluids*; Carbondale, IL., Oct. 15–16, 1991; World Scientific: Singapore, 1992; p 81.
- (5) Davis, L. C. *J. Appl. Phys.* **1992**, *72*, 1334.
- (6) Parthasarathy, M.; Klingenberg, D. J. *Mater. Sci. Eng., R* **1996**, *17*, 57.
- (7) Atten, P.; Foulc, J.-N.; Felici, N. *Int. J. Mod. Phys. B* **1994**, *8*, 2731.
- (8) Atten, P.; Boissy, C.; Foulc, J.-N. *J. Electrostat.* **1997**, *40 & 41*, 3.
- (9) Stangroom, J. E. *J. Intell. Mater. Sys. Struct.* **1996**, *7*, 479.
- (10) Payne, A. R. *J. Appl. Polym. Sci.* **1965**, *9*, 1073.

- (11) Voet, A.; Cook, F. R. *Rubber Chem. Technol.* **1968**, *41*, 1207.
- (12) Martin, J. E.; Odinek, J. *Phys. Rev. Lett.* **1995**, *75*, 2827.
- (13) Adolf, D.; Garino, T.; Hance, B. *Langmuir* **1995**, *11*, 313.
- (14) Ishino, Y.; Maruyama, T.; Ohsaki, T.; Endo, S.; Saito, T.; Goshima, N. *Polym. Prepr.* **1994**, *35* (2), 354.

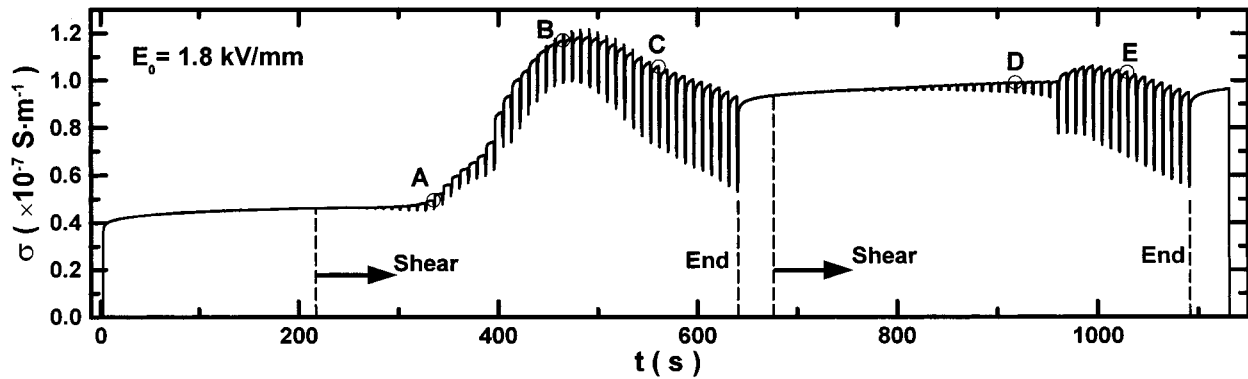


Figure 2. Variation of the suspension conductivity σ with time t under a dc electric field of $E_0 = 1.8$ kV/mm (starting from several seconds prior to turning on the field). The same (oscillatory) torque ramp is performed twice to generate oscillatory shear on the suspension sample.

volume fraction of solids (as determined by centrifugation at 2000*g* for 30 min) is approximately 67%.

A Carri-Med controlled-stress rheometer CSL²500 (TA Instruments) has been modified to impose orthogonal electric and shear fields on the suspension sample. A stainless steel parallel-plate geometry is employed, with a radius of $r_0 = 20.0$ mm. The suspension sample is contained within the gap ($h = 1.00$ mm) between the two parallel plates which also serve as the two electrodes. Qualitatively similar results to those described in this Letter have also been obtained in a cylindrical Couette cell with a gap of 1.00 mm or the parallel-plate geometry with a gap of 0.50 mm. A shear deformation is produced by rotating the upper plate under the action of an axial torque from the rheometer. A Tektronix PS280 dc power supply combined with a Trek 10/10 amplifier is used to generate the desired electric field which is held constant at $E_0 = 1.8$ kV/mm in this study. To measure the conductivity of the suspension, a resistor of $R = 29.8$ k Ω is connected in series into the circuit, in a configuration similar to that used in previous studies.¹⁰ The voltage drop U over this resistor is captured at a rate of 100 samples/s by a Macintosh computer equipped with a National Instruments Lab-NB I/O board. Over 98% of the total voltage drop occurs across the ER fluid, and the conductivity is calculated according to $\sigma = U/\pi r_0^2 R E_0$. Finally, a capacitor of 0.1 μ F is connected in parallel to the resistor to reduce the noise level in U without distorting the signal form of interest to this study.

After being loaded into the measurement geometry, the suspension sample is first (pre)sheared at 400 s^{-1} for 4 min; it is then allowed to equilibrate for 4 min before an oscillatory torque ramp is performed. The electric field is applied 30 s after finishing the preshear, when inertial effects in the rotating fixture have decayed. During the torque ramp, the amplitude T_a of the oscillatory torque ($T = T_a \cos \omega t$) is set to increase linearly from 400 to 22500 μ N·m in 50 discrete steps (here $\omega = 9.40$ rad/s). At each torque amplitude, two cycles of oscillation are performed; however only the strain waveform during the second cycle is captured by the computer driving the rheometer. The torque value is converted to a corresponding stress value using known geometric dimensions ($\tau = 7.958 \times 10^4 T$), and G^* is calculated from Fourier analysis of the first harmonic information according to $\gamma = (\tau_a/G) \cos \omega t + (\tau_a/G') \sin \omega t$. Shortly after finishing the first torque ramp, and without a second preshear, the same torque ramp is repeated once to investigate the effects of shear-induced structural variations in the material.

Figure 2 demonstrates the continuous variation of the conductivity with time for the whole experiment. As a

reference, under an applied dc field of $E_0 = 2.0$ kV/mm, the conductivity of the upper layer of clear liquid from the ER fluid after most of the particles has settled into the bottom layer under gravity is measured to be 2.0×10^{-10} $S \cdot m^{-1}$.

After the electric field is switched on, the conductivity of the ER fluid under static conditions exhibits a gradual increase with time; e.g., compared with the conductivity value measured at 2 s after an electric field of 2.0 kV/mm is applied, the conductivity at 600 s is 18% larger and increases by a total of 20% at 1200 s.

Symmetry arguments suggest that one cycle of mechanical oscillation will be "rectified" into two cycles of variation in electrical conductivity. At each step during the torque ramp, we define a maximum conductivity σ_{max} as the conductivity immediately before starting the strain deformation, and a minimum conductivity σ_{min} as the minimum conductivity detected during the two cycles of imposed mechanical oscillation.

The simultaneous variations in the dynamic modulus G^* and the conductivity as characterized by σ_{max} and σ_{min} with increasing strain amplitude γ_a are displayed in Figure 3. Here G_1^* ($=G_1' + iG_1''$) and G_2^* denote the dynamic modulus measured during the first and second torque ramp, respectively. Both G_1^* and G_2^* are normalized with respect to G_{1max}' , which is the maximum elastic modulus detected during the first torque ramp at small γ_a . Immediately before the first torque ramp is started, the conductivity is $\sigma_0 = 4.6 \times 10^{-8}$ $S \cdot m^{-1}$, and both σ_{max} and σ_{min} are normalized with respect to σ_0 .

From Figure 3a, it is obvious that for $\gamma_a \leq 0.05$ the elastic modulus drops rapidly with increasing γ_a whereas the conductivity exhibits little variation. At $\gamma_a = 0.051$, $(G_1' - G_{1max}')/G_{1max}' = -98\%$; by contrast, $(\sigma_{max} - \sigma_{min})/\sigma_0 = 8.3\%$. Nevertheless, both σ_{max} and σ_{min} keep rising significantly when γ_a is increased further. The ratio σ_{max}/σ_0 reaches its maximum value of 2.6 at $\gamma_a = 10$, and σ_{min}/σ_0 reaches its maximum value of 2.2 at $\gamma_a = 5.7$. Both ratios subsequently decrease with increasing γ_a . At the last step of this initial torque ramp, $\gamma_a = 92$, $\sigma_{max}/\sigma_0 = 2.0$, and $(\sigma_{max} - \sigma_{min})/\sigma_0 = 87\%$.

The significant rise in conductivity as described above must originate from a shear-induced structural variation inside the electrified ER suspension. This is further evidenced by results obtained from the second torque ramp shown in Figure 3b. No preshear is performed between the two ramps, hence the resulting structure in the suspension from the first torque ramp is preserved without disruption. At small γ_a (< 0.02), similar to that shown in Figure 3a, G_2' drops rapidly with increasing γ_a while the variation in σ is insignificant; however, G_2' has now become

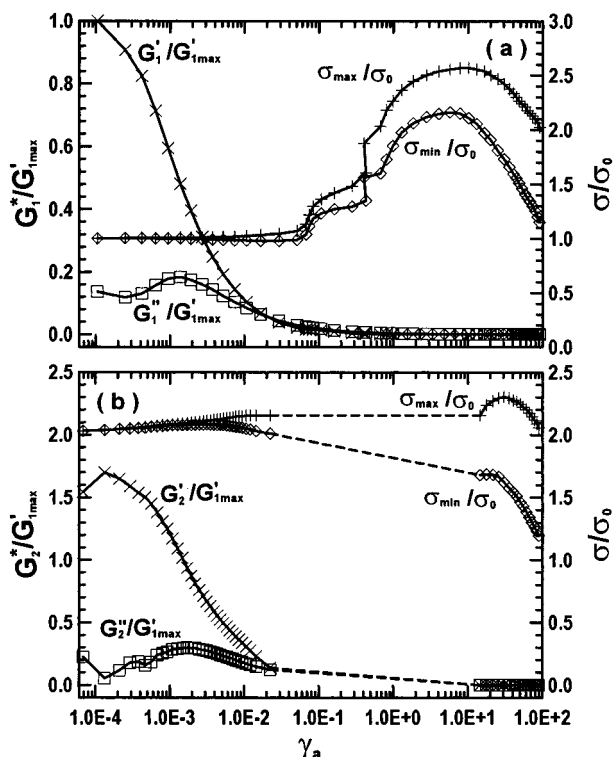


Figure 3. Variations of mechanical modulus ($G^* = G' + iG''$) and electrical conductivity (σ_{\max} and σ_{\min}) of the ER suspension with oscillatory shear strain amplitude γ_a : (a) results obtained from the first torque ramp; (b) results obtained from the second torque ramp. Here, G' and G'' are all normalized with respect to $G'_{1\max} = 3.0 \times 10^5$ Pa, σ_{\max} and σ_{\min} are normalized with respect to $\sigma_0 = 4.6 \times 10^{-8}$ S·m $^{-1}$.

substantially larger, with a maximum enhancement of $G''_2/G'_{1\max} = 1.7$. Moreover, a sudden jump in γ_a from $\gamma_a = 0.022$ to $\gamma_a = 15$ is observed as T_a is increased from 1.53×10^4 to 1.57×10^4 $\mu\text{N}\cdot\text{m}$, indicating the onset of a catastrophic structural breakdown inside the sample beyond a certain critical shear stress. At strains above $\gamma_a = 15$, σ_{\max} increases slightly until a maximum is reached and then decreases monotonically.

The above observations are dissimilar to those for carbon-black-filled rubbers.¹⁰ Obviously in rubbers the medium surrounding the carbon black particles is extremely viscous, and this seriously hinders pronounced structural rearrangement in the material.

Initial comparison of the results shown in parts a and b of Figure 3 at small γ_a suggests that a significantly enhanced rigidity of the ER suspension is accompanied by a substantial rise in its conductivity; however, further measurements show that an aggregated state with a larger conductivity does *not* necessarily lead to an enhanced rigidity. For example, when we reverse the direction of the first torque ramp, i.e., starting from the largest T_a , and perform a second torque ramp as described before, the material properties of the resulting structure are markedly different. A larger maximum in σ_{\max}/σ_0 ($=3.5$) is attained shortly after the second ramp is commenced; however the maximum in G' detected during either ramp is of similar magnitude to $G'_{1\max}$ shown in Figure 3a. No jump in γ_a appears during the second ramp. These changes highlight the sensitivity of the suspension structure to the shear history. Construction of hysteresis plots in (G', σ) space is very helpful in displaying these path-dependent material properties.

Representative waveforms of strain $\gamma(t)$ and conductivity $\sigma(t)$ during oscillation are displayed in Figure 4. Their

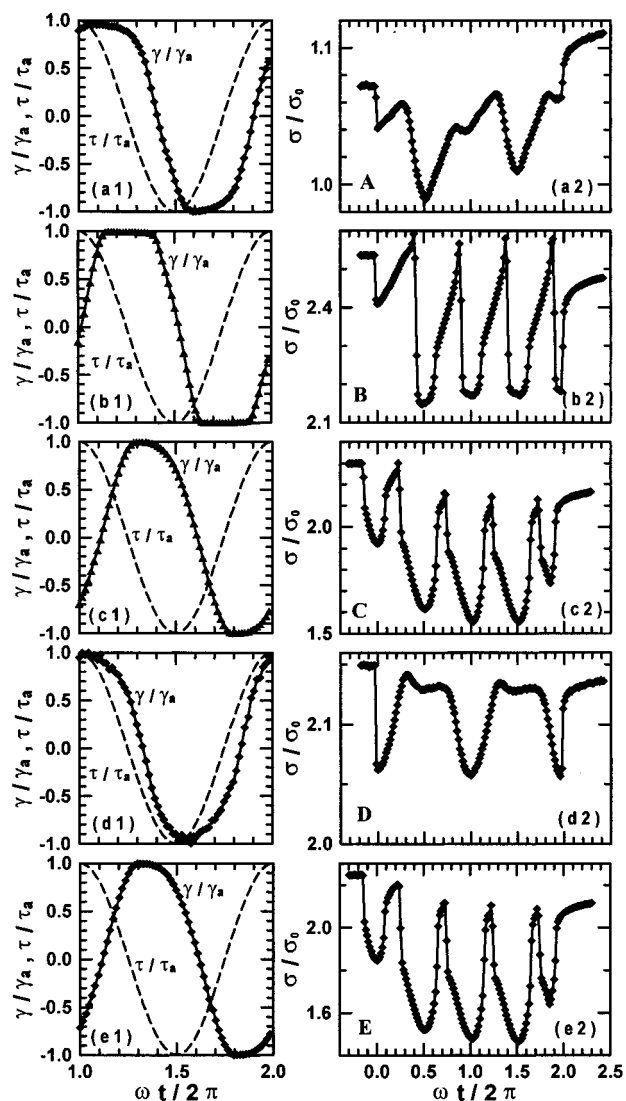


Figure 4. Detailed strain $\gamma(t)$ and conductivity $\sigma(t)$ waveforms at times indicated by circles from A to E in Figure 2. At each location, two cycles of mechanical oscillation are generated, while the conductivity waveform during the second cycle is captured. The dashed cosine curves indicate the imposed oscillatory stress $\tau = \tau_a \cos \omega t$ with $\omega = 9.40$ rad/s. γ , τ , and σ are normalized with γ_a , τ_a , and σ_0 , respectively. (a1) and (a2) A, $\tau_a = 534$ Pa, $\gamma_a = 0.051$; (b1) and (b2) B, $\tau_a = 1073$ Pa, $\gamma_a = 4.1$; (c1) and (c2) C, $\tau_a = 1468$ Pa, $\gamma_a = 45$; (d1) and (d2) D, $\tau_a = 1073$ Pa, $\gamma_a = 0.0094$; (e1) and (e2) E, $\tau_a = 1539$ Pa, $\gamma_a = 51$.

corresponding temporal locations in Figure 2 have been marked by circles from A to E, respectively. During the first torque ramp, the disruption to the suspension structure is still not severe at A ($\gamma_a = 0.051$), while grave structural disruptions occur at both B ($\gamma_a = 4.1$) and C ($\gamma_a = 45$); during the second ramp, only small deformation is generated at D ($\gamma_a = 0.0094$), and total structural breakdown arises at E ($\gamma_a = 51$).

By design, the rheometer exerts an oscillatory torque of the form $T = T_a \cos \omega t$. Due to the small, yet finite, inertial rise time for the imposed torque to jump from 0 to T_a at the beginning, in plotting Figure 4 we generally assume that the first maximum in T generates a maximum disturbance to the structure in the sample and corresponds to the first minimum in conductivity. This is not always strictly correct, as is evidenced by the time mismatch observable in Figure 4 (c2) and (e2). From Figures 4 and 2 it is clear that before performing each new oscillation

step the conductivity has recovered sufficiently from the disturbance induced by previous oscillation step.

In comparison with the strain waveforms, the conductivity waveforms are much more complicated and are typically asymmetric. Although it is difficult to analyze the conductivity response in detail, some characteristics are readily discernible. The asymmetry between the two cycles of variation in σ during one cycle of mechanical oscillation is most pronounced at small γ_a , as is clearly demonstrated in Figure 4 (a2) and (d2). When the internal suspension structure is completely destroyed at large deformations, similar strain and conductivity waveforms should be observed regardless of the sample's previous shear history, as is confirmed by comparing Figure 4 (c1) and (c2), and (e1) and (e2). At large γ_a , notable asymmetry also exists between the decreasing portion (corresponding to structure breakdown) and the increasing portion (corresponding to structure reformation) of the conductivity cycle, as can be seen from Figure 4 (b2) and (c2). In carbon-black-reinforced vulcanizates, asymmetrical waveforms of conductivity have also been observed for high loadings of "high structure black".¹¹

Careful examination of the corresponding strain waveform and conductivity waveform shown in Figure 4 suggests that the minimum in σ coincides with the maximum shear strain at low γ_a but coincides with the maximum shear rate at high γ_a . Similar conclusions on the variation of dielectric constant under oscillatory shear have also been obtained.¹³

Discussion. First of all, it is clear from Figure 3 that at small γ_a , no matter how different the unperturbed basic suspension structures are, there is no direct correlation between G' and σ . The elastic modulus G' certainly depends on field-induced interactions among particles and the resulting columnar structures; however, the mechanisms for electrical conduction through ER materials under strong electric fields, especially the physicochemical processes involved in the narrow gap between neighboring particles, are poorly understood at present. The possibility of conduction via electron tunneling has been negated for some carbon-black-filled polymers (tested in dc fields up to ~ 1 kV/mm)¹⁵ and has also been argued against for ER suspensions.³ With some *experimental justification*, a conduction model has recently been proposed for the ER response under dc or low-frequency ac fields.^{7,8} In this model, the passage of current through the particle chain determines the electric field and surface charge distributions giving rise to the attractive force between particles. Hence a direct correlation between the interparticle attractive force and the current through the chain is expected. However, a more quantitative analysis of this model (see Figures 8 and 9 in ref 16) for a specific set of material parameters reveals that the chain conductivity decreases *more rapidly* with increasing separation of particles along the chain than the attractive force between two particles. The experimental observations in Figure 3 are in direct contrast to the above expectations. It is possible that the suspension we have used is too concentrated for this simple chain model to be applicable.

Oscillatory shear with large γ_a causes radical changes in the overall suspension structure. Since the highly concentrated suspension is optically opaque, we have not, as yet, been able to probe the internal structure directly

and here we simply review some recent related findings which may help in advancing theoretical understanding of the observed ER response.

Noting the significant enhancement in G' detected early during the second torque ramp after large-amplitude oscillatory shear in the first ramp, it is immediately tempting to associate our results with the formation of sheet structures observed in a suspension of 10 vol % silica particles in silicone oil.¹⁷ However, Brownian dynamics simulations¹⁸ reveal that such structured microphase separation may not emerge in highly concentrated suspensions as used herein. Furthermore, we have performed some additional tests (with differing constant T_a) that show significant structural variation can only be induced by oscillatory shear with strain amplitudes beyond a critical value (ca. 10%). In such cases even the first cycle of oscillation upon starting the test can raise the conductivity by a factor of 2 or more. By contrast, complete formation of the sheet structures observed previously took at least a few minutes ($\gamma_a = 1.0$, $\omega = 188.5$ rad/s).¹⁷

In addition to the intrinsic material properties of the two phases, interparticle *contacts*, as determined by geometrical considerations of particle packing in a dense suspension, must also be of importance to the material properties of ER suspensions. This can be exemplified by considering an imaginary concentrated suspension of small identical circular disks of finite thickness. Several extreme ways of arranging the disks into structures spanning the electrodes can be easily identified in which the contacts among disks are either mostly edge-to-face or purely face-to-face or purely edge-to-edge. Under a strong electric field, these different ways of particle packing in the suspension will undoubtedly lead to substantially different mechanical rigidity and electrical conductivity of the suspension. To radically change the manner of particle packing, imposition of a strong external deformation is required.

It is well-known now that the *network of contacts*¹⁹ is typically inhomogeneous in granular materials due to various geometric defects of the particles. This crucially affects the stress transfer properties of granular media. Irregular networks of force-chains have been observed for transmitting compressive loading stresses.^{20,21} Defects in contact may also play an important role in the early stages of failure in ER materials and can be understood in the context of the anisotropic network microstructure model recently proposed.²² As the shear deformation is increased, the secondary cross-linking chains will break down first due to the extremely nonuniform distribution of the extensional strain. However, the loss of such secondary chains will not dramatically affect the material conductivity. At progressively larger strains, the weaker primary chains with defects in contact fail followed by all the remaining chains. During this yielding process, the stress distribution continuously adjusts to accompany the dynamic structural variation.

In summary, simultaneous measurements of dynamic modulus and electrical conductivity have been performed for a highly concentrated ER suspension under a strong dc electric field. Measurements at small γ_a reveal that

(15) Cashell, E. M.; Coey, J. M. D.; Wardell, G. E.; McBrierty, V. J. *J. Appl. Phys.* **1981**, *52*, 1542.

(16) Tang, X.; Wu, C.; Conrad, H. *J. Appl. Phys.* **1995**, *78*, 4183.

(17) Bossis, G.; Grasselli, Y.; Lemaire, E.; Persello, J.; Petit, L. *Europhys. Lett.* **1994**, *25*, 335.

(18) Melrose, J. R.; Heyes, D. M. *J. Chem. Phys.* **1993**, *98*, 5873.

(19) Roux, S.; Bideau, D.; Hansen, A. In *Disorder and Granular Media*; Bideau, D., Hansen, A., Eds.; North-Holland: Amsterdam, 1993; p 299.

(20) Travers, T.; Ammi, M.; Bideau, D.; Gervois, A.; Messenger, J. C.; Troadec, J. P. *Europhys. Lett.* **1987**, *4*, 329.

(21) Liu, C.-h.; Nagel, S. R.; Schecter, D. A.; Coppersmith, S. N.; Majumdar, S.; Narayan, O.; Witten, T. A. *Science* **1995**, *269*, 513.

(22) Pan, X.-D.; McKinley, G. H. *Appl. Phys. Lett.* **1997**, *71*, 333.

there is no direct correlation between G' and σ of the suspension. Oscillatory shear with large γ_a leads to radical changes in the suspension microstructure that affect both the mechanical strength and electrical conductivity of the material. These results suggest that optimizing contacts among particles and between particles and electrodes may be an important means of designing better ER materials. Further studies are needed on the variation in ER response arising from the type of contact between two particles,

i.e., point contact vs plane contact, as well as from the homogeneity of the network of contacts.

Acknowledgment. This work was supported by the National Science Foundation under Grant No. DMR-9400396. X.-D. Pan is indebted to Dr. Yuan Z. Lu, Mr. T. Deng, Dr. G. Braithwaite, and Mr. M. T. Arigo for their technical support.

LA9711084